Reduction of single-walled carbon nanotube diameter to sub-nm via feedstock

Theerapol Thurakitseree[1], Christian Kramberger[2], Pei Zhao[1], Shohei Chiashi[1], Erik Einarsson[1,3], and Shigeo Maruyama[*,1]

[1] Department of Mechanical Engineering, The University of Tokyo, 7-3-1 Hongo, Bunkyo-ku, Tokyo, 113-8656, Japan
[2] Faculty of Physics, University of Vienna, Strudlhofgasse 4., Vienna, A-1090, Austria
[3] Global Center of Excellence for Mechanical Systems Innovation, The University of Tokyo, 7-3-1 Hongo, Bunkyo-ku, Tokyo, 113-8656, Japan

Received XXXXXX, revised XXXX, accepted XXXX
Published online XXXX

Key words: Single-walled carbon nanotube, vertically aligned, diameter control, acetonitrile, nitrogen-doping
PACS 81.07.De

[*] Corresponding author: e-mail maruyama@photon.t.u-tokyo.ac.jp, Phone: +81-3-5841-6421, Fax: +81-3-5800-6983

Vertically aligned single-walled carbon nanotube arrays were synthesized from dip-coated binary Co/Mo catalyst by no-flow chemical vapor deposition from either pure ethanol or acetonitrile as carbon feedstock. By changing to acetonitrile the mean diameter was reduced from 2.1 nm to less than 1.0 nm despite using identically prepared catalyst. The demonstrated diameter control on flat substrates is a versatile approach towards the direct synthesis of tailored single-walled carbon nanotubes.

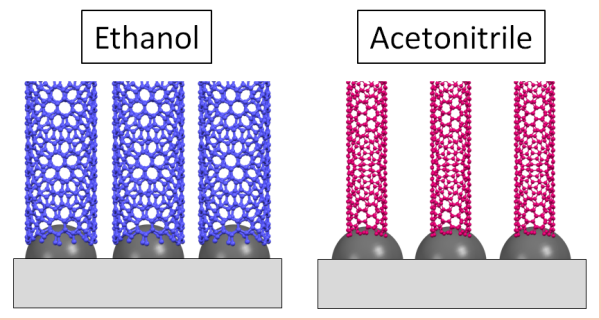

1 Introduction Single-walled carbon nanotubes (SWNTs) are a promising novel material for future electronic applications such as flexible thin-film field effect transistors [1–5]. Depending on their chirality, SWNTs can either be metallic or semiconducting [6]. Since the mean diameter limits the number of possible chiralities, diameter control is a prerequisite to obtaining bulk SWNTs with homogeneous properties. Hence, direct tuning of diameter during the SWNT growth process is a necessity. Conventionally, this has been achieved by controlling the catalyst particle size during synthesis [7–11]. The SWNT diameter can be reduced by decreasing the growth temperature during synthesis by chemical vapor deposition (CVD) [7,8], which is generally attributed to less efficient sintering of metal catalyst nanoparticles.

In this study, we demonstrate that the mean diameter of SWNTs can be changed by incorporating nitrogen (N) during the growth process, and is independent of catalyst size. Vertically aligned (VA-) SWNTs grown from identically prepared cobalt/molybdenum (Co/Mo) binary catalysts were synthesized using pure ethanol or pure acetonitrile as C and/or N sources by no-flow CVD. The mean SWNT diameter was reduced from 2.1 nm to less than 1 nm when using acetonitrile. Our results suggest that nitrogen takes an active role at the interface between the catalyst particle and the nanotube wall. The interaction of N and Co (N-Co) is stronger than that of C and Co (C-Co),

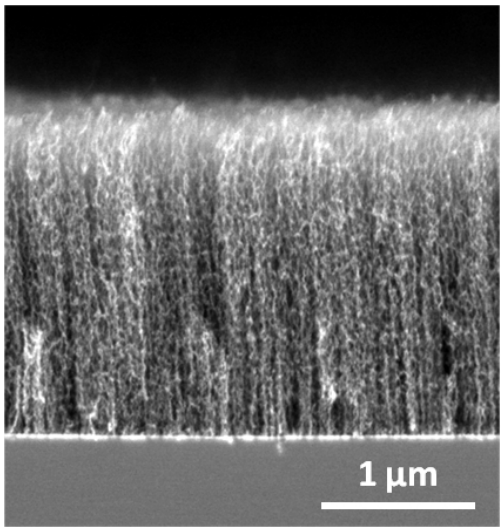

Figure 1 SEM image of a VA-SWNT array synthesized by no-flow acetonitrile CVD.

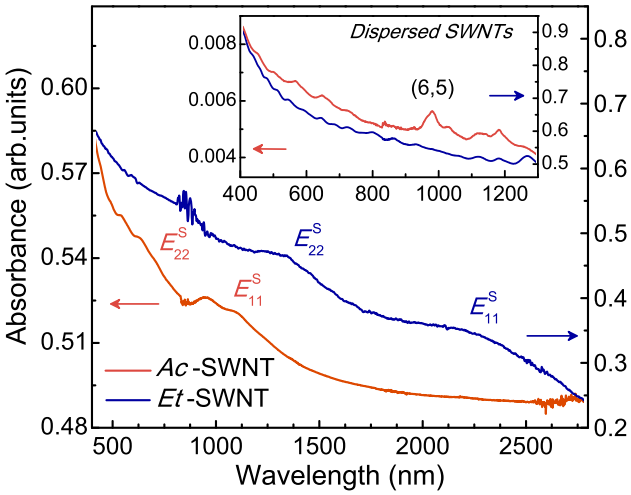

Figure 2 Optical absorption spectra of as-grown VA-SWNTs synthesized with different feedstocks show a dramatic difference in the first optical transition energies E_{11} [15]. The inset shows spectra from SWNTs dispersed in D_2O using DOC as a surfactant. Red and blue lines represent acetonitrile (*Ac*) and ethanol (*Et*) CVD samples, respectively.

thus leading to small-diameter SWNTs originating from the same catalyst particles [12].

2 Experimental

2.1 Synthesis Arrays of VA-SWNTs were synthesized on quartz substrates by no-flow chemical vapor deposition (CVD) [13]. The Co/Mo binary catalyst particles were prepared by dip-coating quartz substrates [14] in Mo-acetate and Co-acetate solutions containing 0.1 wt.% metal content. During heating of the CVD furnace, the catalysts were reduced under flowing Ar containing 3% H_2. After reaching 800°C, 40 μL of either pure ethanol (C_2H_5OH) or pure acetonitrile (CH_3CN) was introduced as carbon and nitrogen sources. The CVD reaction was performed for 3 min at a pressure of 1.7 to 2.3 kPa. The ethanol- and acetonitrile-grown SWNTs are hereafter referred to as *Et*-SWNT and *Ac*-SWNT, respectively. Optionally, as-grown VA-SWNTs were dispersed in D_2O containing 1 wt.% of sodium deoxycholate (DOC) surfactant. Following 10 min of bath sonication and additional 30 min of horn-type ultrasonication (UP-400S, Hielscher Ultrasonics), dispersed SWNTs were centrifuged at 85 000 rpm (327 000 *g*) for 30 min before the supernatant was extracted.

2.2 Characterization The vertically aligned morphology of as-grown SWNTs was characterized by scanning electron microscopy (SEM). The diameter of VA-SWNT arrays was evaluated by UV-vis-NIR absorption spectroscopy, resonance Raman spectroscopy using excitation wavelengths of 488, 514, and 633 nm, and transmission electron microscopy (TEM). For photoluminescence excitation (PLE) spectra, the fluorescence emission was recorded from 910 to 1370 nm, and the excitation was scanned from 500 to 830 nm in 5 nm steps.

3 Results and discussion Ethanol is a well-established carbon source for SWNT synthesis [16,17]. Figure 1 clearly shows the capability of acetonitrile to act as a source for VA-SWNT synthesis [18]. The film thickness is found to be thinner than for VA-SWNTs synthesized from conventional alcohol catalytic CVD [18]. Optical absorption spectra are shown in Fig. 2. The first optical transitions (E_{11}) are observed at 2250 nm (0.55 eV) and 1000 nm (1.24 eV) for *Et*- and *Ac*-SWNTs, respectively. The mean diameters of the samples were evaluated using the empirical Kataura plot reported in [19], and are 2.1 and 0.8 nm for *Et*-SWNTs and *Ac*-SWNTs, respectively.

Figure 3 shows resonance Raman spectra of as-grown SWNTs synthesized from both ethanol and acetonitrile. The diameters were evaluated from the RBM region using the following empirical relation [19], $\omega_{\mathrm{RBM}} = 217.8/d$ [nm]$+15.7$. In the empirical Kataura plot [19] the 488 and 514 nm energies excite the first metallic resonance of 0.8 nm *Ac*-SWNTs. The 633 nm excitation wavelength excites the semiconducting resonance in *Ac*-SWNTs. For 2.1 nm *Et*-SWNTs all three excitations lie in the intermingled bands of E_{33} and E_{44} optical transitions. The strong BWF lineshape in the G-band of *Ac*-SWNTs for 488 and 514 nm excitation is a hallmark of metallic resonance. The position of the G^+-band is 1594 cm^{-1} for all excitations in both samples. RBM peaks confirm selective resonances with diameters between 0.8 and 1.0 nm in *Ac*-SWNTs and between 1.2 and 2.3 nm in *Et*-SWNTs.

In the metallic resonance at 488 nm excitation, a large increase in D-band intensity is observed for *Ac*-SWNTs (Fig. 3). The G/D ratios at this excitation wavelength in the *Et*- and *Ac*-SWNTs are 19.8 and 3.2, respectively. The

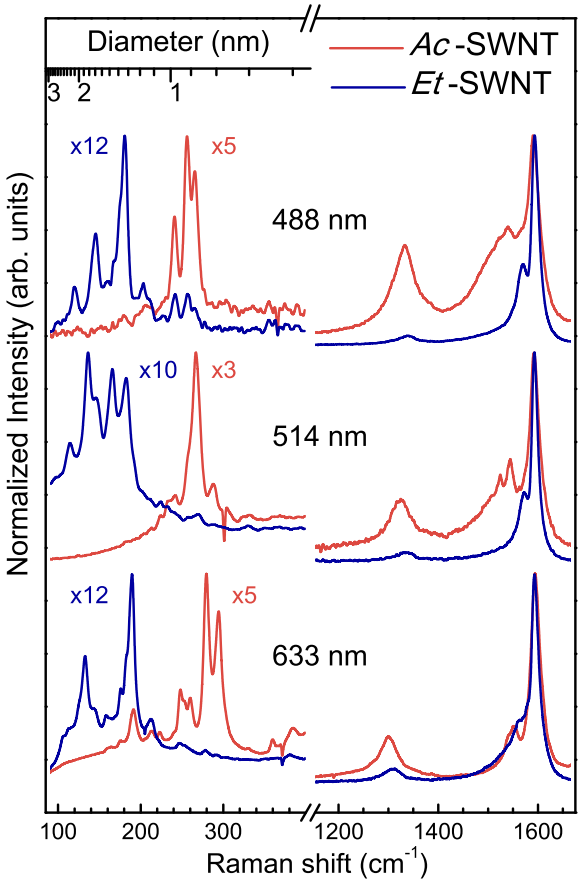

Figure 3 Resonance Raman spectra obtained using three different excitation wavelengths from acetonitrile (*Ac*)- and ethanol (*Et*)-grown SWNTs.

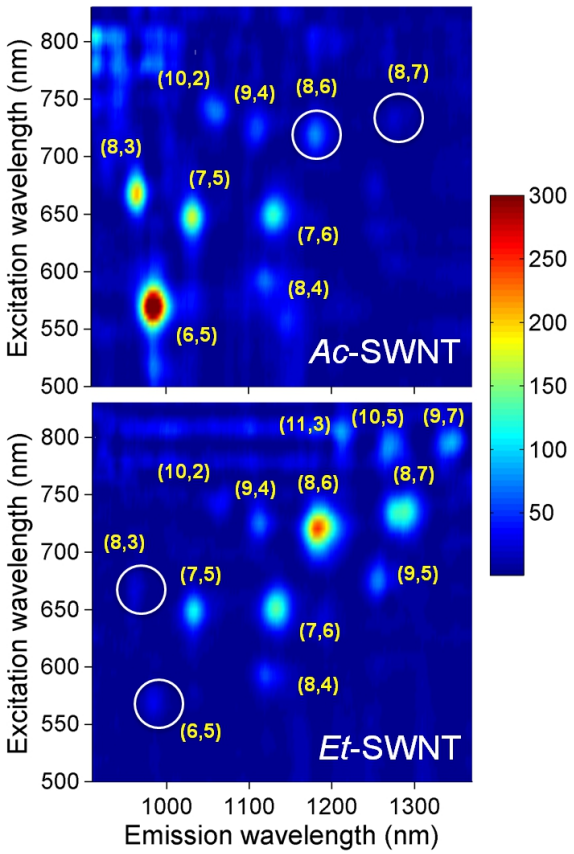

Figure 4 Photoluminescence excitation (PLE) maps of acetonitrile (*Ac*)- and ethanol (*Et*)-grown SWNTs measured from the same dispersed SWNTs as measured in optical absorption (Fig. 2 inset).

large D-band is primarily due to defects corresponding to kink structures observed by TEM [15]. The higher curvature of small-diameter *Ac*-SWNTs [20] may contribute to the large D-band. The linear dependence of D-band frequency dispersion on excitation laser energy (E_{laser}) has been previously reported [20]. Reference [20] also reports a downshift of the D-band frequency for narrow-diameter SWNTs. We observed an offset of 10 cm^{-1} in D-band frequency in *Ac*-SWNTs for all three E_{laser} measurements (Fig. 3). We also observe an offset of 41 cm^{-1} in G′-band frequency (not shown). This is in agreement with Raman studies on different diameter sizes of inner and outer walls in double-walled carbon nanotubes [21].

PLE maps of dispersed *Ac*-SWNTs and *Et*-SWNTs are presented in Fig. 4. Each peak in the PLE map corresponds to an E_{22} absorption and an E_{11} emission by one semiconducting chirality. For *Ac*-SWNTs the peak intensities are clustered at shorter excitation and emission wavelengths, whereas in *Et*-SWNTs they are strongest at longer wavelengths. The markings for individual chiralities in Fig. 4 reveal clear-cut differences in the relative population between dispersed *Ac*-SWNTs and *Et*-SWNTs. The peak positions are found to be indistinguishable. The strongest peaks for *Ac*-SWNTs stem from (6,5), (8,3), (7,5), and (7,6) nanotubes, whereas (8,6), (8,7), (7,6) and (7,5) nanotubes are dominant for *Et*-SWNTs. The diameters accessible by PLE mapping are limited by the narrow semiconducting window and the centrifugation step, which enriches the population of small-diameter SWNTs [22]. The shift in PLE intensities from longer to shorter wavelengths for *Et*-SWNTs and *Ac*-SWNTs is therefore only reminiscent of—but no longer quantitative to—the diameter shift from 2.1 to 0.8 nm in the as-grown *Et*-/*Ac*-SWNTs.

These findings of very different diameters of nanotubes within VA-SWNT arrays synthesized from acetonitrile and ethanol demonstrate that changes in SWNT diameter can be achieved without any changes in catalyst preparation. Furthermore, our finding that nanotubes of very different diameters can be synthesized within the same VA-SWNT array by changing the carbon precursor demonstrates that the SWNT diameter can be substantially changed without altering the catalyst preparation.

Several possible scenarios can be considered for this achievement of SWNTs with drastically smaller

diameters. The DFT calculation in Ref. [12] indicates stronger bonding between the Co nanoparticle and nitrogen than with carbon. Hence, it can be assumed that N-containing graphene surrounding a Co nanoparticle would have stronger adhesion to the nanoparticle than pristine graphene. The favorable *weak* adhesion during the nanotube nucleation process has been previously investigated using molecular dynamics simulation studies [23,24]. It was reported that the reduction of nanotube diameter can be obtained when the adhesion between C and the catalyst nanoparticle is reduced [24]. The discussion in Ref. [25], however, suggests *stronger* adhesion should enhance the selectivity of smaller diameter SWNTs by causing the nanotube wall to grow perpendicular to the catalyst particle surface. Despite being a less favorable growth condition, this mechanism is unrelated to the size of the nanoparticle [26].

Another possibility for the reduced diameter is a reaction between N and the Co nanoparticles, forming a structure similar to Co_xN_y [27]. Due to the strong interaction of N with the nanoparticle surface, surface diffusion of C would be hindered, leaving only the bulk diffusion route for nanotube formation, which corresponds to smaller diameter SWNTs.

4 Summary We address diameter control of SWNTs in the range of 2 to 1 nm via the choice of the carbon feedstock. The same Co/Mo binary catalyst particles yield vertically aligned arrays with mean diameters of 2.1 nm from ethanol and 0.8 nm from acetonitrile. The difference in diameters is evidenced by optical absorption and resonance Raman spectroscopy obtained using three different excitation lasers. PLE mapping also shows a shift to narrower chiralities. While the choice of either ethanol or acetonitrile as a carbon source for CVD synthesis is an effective way to control SWNT diameters, the microscopic understanding of how the feedstock can affect the diameter of the growing SWNTs deserves further studies.

Acknowledgements Part of this work was financially supported by Grants-in-Aid for Scientific Research (19054003, 22226006, 23760180 and 23760179), and the Global COE Program "Global Center for Excellence for Mechanical Systems Innovation". TT acknowledges support from the Higher Educational Strategic Scholarships for Frontier Research Network (CHE-PhD-SFR) granted by the Office of Higher Education Commission, Thailand. CK acknowledges the Austrian Academy of Sciences for the APART fellowship A-11456.

References

[1] Q. Cao, H. S. Kim, N. Pimparkar, J. P. Kulkarni, C. Wang, M. Shim, K. Roy, M. A. Alam, and J. A. Rogers, Nature **454**, 495 (2008).
[2] E. Artukovic, M. Kaempgen, D. S. Hecht, S. Roth, and G. Grüner, Nano Lett. **5**, 757 (2005).
[3] F. N. Ishikawa, H. K. Chang, K. Ryu, P. C. Chen, A. Badmaev, L. G. De Arco, G. Shen, and C. Zhou, ACS Nano **3**, 73 (2009).
[4] W. J. Yu, S. Y. Lee, S. H. Chae, D. Perello, G. H. Han, M. Yun, and Y. H. Lee, Nano Lett. **11**, 1344 (2011).
[5] D. M. Sun, M. Y. Timmermans, Y. Tian, A. G. Nasibulin, E. I. Kauppinen, S. Kishimoto, T. Mizutani, and Y. Ohno, Nat. Nanotechnol. **6**, 156 (2011).
[6] M. S. Dresselhaus, G. Dresselhaus, R. Saito, and A. Jorio, Physics Reports **409**, 47 (2005).
[7] S. M. Bachilo, L. Balzano, J. E. Herrera, F. Pompeo, D. E. Resasco, and R. B. Weisman, J. Am. Chem. Soc. **125**, 11186 (2003).
[8] Y. Miyauchi, S. Chiashi, Y. Murakami, Y. Hayashida, and S. Maruyama, Chem. Phys. Lett. **387**, 198 (2004).
[9] S. Lee, C. Z. Loebick, L. D. Pfefferle, and G. L. Haller, J. Phys. Chem. C **115**, 1014 (2011).
[10] E. Dervishi, Z. Li, F. Watanabe, Y. Xu, V. Saini, A. R. Biris, and A. S. Biris, J. Mater. Chem. **19**, 3004 (2009).
[11] S. H. Lee and G. H. Jeong, Electronic Materials Letters **8**, 5 (2012).
[12] J. P. O'Byrne, Z. Li, S. L. T. Jones, P. G. Fleming, J. A. Larsson, M. A. Morris, and J. D. Holmes, ChemPhysChem **12**, 2995 (2011).
[13] R. Xiang, Z. Zhang, K. Ogura, J. Okawa, E. Einarsson, Y. Miyauchi, J. Shiomi, and S. Maruyama, Jpn. J. Appl. Phys. **47**, 1971 (2008).
[14] Y. Murakami, Y. Miyauchi, S. Chiashi, and S. Maruyama, Chem. Phys. Lett. **377**, 49 (2003).
[15] T. Thurakitseree, C. Kramberger, P. Zhao, S. Aikawa, S. Harish, S. Chiashi, E. Einarsson, and S. Maruyama, Carbon **50**, 2635 (2012).
[16] Y. Murakami, Y. Miyauchi, S. Chiashi, and S. Maruyama, Chem. Phys. Lett. **374**, 53 (2003).
[17] S. Maruyama, R. Kojima, Y. Miyauchi, S. Chiashi, and M. Kohno, Chem. Phys. Lett. **360**, 229 (2002).
[18] Y. Murakami, S. Chiashi, Y. Miyauchi, M. H. Hu, M. Ogura, T. Okubo, and S. Maruyama, Chem. Phys. Lett. **385**, 298 (2004).
[19] P. T. Araujo, S. K. Doorn, S. Kilina, S. Tretiak, E. Einarsson, S. Maruyama, H. Chacham, M. A. Pimenta, and A. Jorio, Phys. Rev. Lett. **98**, 067401 (2007).
[20] S. D. M. Brown, A. Jorio, M. S. Dresselhaus, and G. Dresselhaus, Phys. Rev. B **64**, 073403 (2001).
[21] R. Pfeiffer, H. Kuzmany, F. Simon, S. N. Bokova, and E. Obraztsova, Phys. Rev. B **71**, 155409 (2005).
[22] P. Zhao, E. Einarsson, R. Xiang, Y. Murakami, and S. Maruyama, J. Phys. Chem. C **114**, 4831 (2010).
[23] M. A. Ribas, F. Ding, P. B. Balbuena, and B. I. Yakobson, J. Chem. Phys. **131**, 224501 (2009).
[24] F. Ding, P. Larsson, J. A. Larsson, R. Ahuja, H. Duan, A. Rosen, and K. Bolton, Nano Lett. **8**, 463 (2008).
[25] J. H. Hafner, M. J. Bronikowski, B. R. Azamian, P. Nikolaev, A. G. Rinzler, D. T. Colbert, K. A. Smith, and R. E. Smalley, Chem. Phys. Lett. **296**, 195 (1998).
[26] M. F. C. Fiawoo, A. M. Bonnot, H. Amara, C. Bichara, J. Thibault-Pénisson, and A. Loiseau, Phys. Rev. Lett. **108**, 195503 (2012).
[27] M. Matsuoka, K. Ono, and T. Inukai, Appl. Phys. Lett. **49**, 977 (1986).